Monthly Notices
of the
ROYAL ASTRONOMICAL SOCIETY

MNRAS **437,** 1519–1533 (2014)
Advance Access publication 2013 November 13

doi:10.1093/mnras/stt1983

PESSTO monitoring of SN 2012hn: further heterogeneity among faint Type I supernovae★

S. Valenti,[1,2]† F. Yuan,[3,4] S. Taubenberger,[5] K. Maguire,[6] A. Pastorello,[7] S. Benetti,[7] S. J. Smartt,[8] E. Cappellaro,[7] D. A. Howell,[1,2] L. Bildsten,[2,9] K. Moore,[2] M. Stritzinger,[10] J. P. Anderson,[11] S. Benitez-Herrera,[5] F. Bufano,[12] S. Gonzalez-Gaitan,[11] M. G. McCrum,[8] G. Pignata,[12] M. Fraser,[8] A. Gal-Yam,[13] L. Le Guillou,[14] C. Inserra,[8] D. E. Reichart,[15] R. Scalzo,[3] M. Sullivan,[16] O. Yaron[13] and D. R. Young[8]

[1]*Las Cumbres Observatory Global Telescope Network, 6740 Cortona Dr., Suite 102, Goleta, CA 93117, USA*
[2]*Department of Physics, University of California, Santa Barbara, Broida Hall, Mail Code 9530, Santa Barbara, CA 93106-9530, USA*
[3]*Research School of Astronomy and Astrophysics, The Australian National University, Weston Creek, ACT 2611, Australia*
[4]*ARC Centre of Excellence for All-sky Astrophysics (CAASTRO), 44 Rosehill Street Redfern, NSW 2016, Australia*
[5]*Max-Planck-Institut für Astrophysik, Karl-Schwarzschild-Str. 1, D-85741 Garching bei München, Germany*
[6]*Department of Physics (Astrophysics), University of Oxford, DWB, Keble Road, Oxford OX1 3RH, UK*
[7]*INAF Osservatorio Astronomico di Padova, Vicolo dell'Osservatorio 5, I-35122 Padova, Italy*
[8]*Astrophysics Research Centre, School of Mathematics and Physics, Queens University Belfast, Belfast BT7 1NN, UK*
[9]*Kavli Institute for Theoretical Physics, Kohn Hall, University of California, Santa Barbara, CA 93106-4030, USA*
[10]*Department of Physics and Astronomy, Aarhus University, Ny Munkegade 120, DK-8000 Aarhus C, Denmark*
[11]*Departamento de Astronomia, Universidad de Chile, Casilla 36-D, Santiago, Chile*
[12]*Departamento de Ciencias Fisicas, Universidad Andres Bello, Avda. Republica 252, Santiago, Chile*
[13]*Department of Particle Physics and Astrophysics, The Weizmann Institute of Science, Rehovot 76100, Israel*
[14]*UPMC Univ. Paris 06, UMR 7585, Laboratoire de Physique Nucleaire et des Hautes Energies (LPNHE), F-75005 Paris, France*
[15]*University of North Carolina at Chapel Hill, Campus Box 3255, Chapel Hill, NC 27599-3255, USA*
[16] *School of Physics and Astronomy, University of Southampton, Southampton SO17 1BJ, UK*

Accepted 2013 October 14. Received 2013 August 28; in original form 2013 January 30

ABSTRACT

We present optical and infrared monitoring data of SN 2012hn collected by the Public European Southern Observatory Spectroscopic Survey for Transient Objects. We show that SN 2012hn has a faint peak magnitude ($M_R \sim -15.65$) and shows no hydrogen and no clear evidence for helium in its spectral evolution. Instead, we detect prominent Ca II lines at all epochs, which relates this transient to previously described 'Ca-rich' or 'gap' transients. However, the photospheric spectra (from −3 to +32 d with respect to peak) of SN 2012hn show a series of absorption lines which are unique and a red continuum that is likely intrinsic rather than due to extinction. Lines of Ti II and Cr II are visible. This may be a temperature effect, which could also explain the red photospheric colour. A nebular spectrum at +150 d shows prominent Ca II, O I, C I and possibly Mg I lines which appear similar in strength to those displayed by core-collapse supernovae (SNe). To add to the puzzle, SN 2012hn is located at a projected distance of 6 kpc from an E/S0 host and is not close to any obvious star-forming region. Overall SN 2012hn resembles a group of faint H-poor SNe that have been discovered recently and for which a convincing and consistent physical explanation is still missing. They all appear to explode preferentially in remote locations offset from a massive host galaxy with deep limits on any dwarf host galaxies, favouring old progenitor systems. SN 2012hn adds heterogeneity to this

★This paper is based on observations obtained during the first run of the PESSTO. Data from the following telescopes are included: New Technology Telescope(184.D-1140,188.D-3003), Very Large Telescope-UT1(089.D-0270), Panchromatic Robotic Optical Monitoring and Polarimetry Telescopes (PROMPT), TRAnsiting Planets and PlanetesImals Small Telescope (TRAPPIST), DUPONT, MAGELLAN.

† E-mail: svalenti@lcogt.net

sample of objects. We discuss potential explosion channels including He-shell detonations and double detonations of white dwarfs as well as peculiar core-collapse SNe.

Key words: supernovae: general – supernovae: individual: 2012hn.

1 INTRODUCTION

In recent years, an increasing number of new transients with unusual properties have been discovered, thanks to the advent of modern, wide-field optical transient surveys, such as the Texas Supernova Search (Quimby 2006), the Catalina Real-Time Transient Survey (CRTS; Drake et al. 2009), the Palomar Transient Factory (PTF; Rau et al. 2009) and the Panoramic Survey Telescope and Rapid Response System (Kaiser et al. 2002). Many new objects have been found in regions of the time-scale/luminosity parameter space unexplored before (e.g. faint and/or fast evolving transients) or were located in regions of the sky undersampled by traditional *targeted* surveys (transients in faint hosts or in the outskirts of bright galaxies).

Driven by their observed characteristics, attempts have been made to arrange these novel transients in new classes, trying also to revise the classification of historical supernovae (SNe) in the context of non-standard scenarios. In particular, major efforts have been made to theoretically explain new transients that may not be due to the canonical mechanisms of iron core-collapse or the thermonuclear explosion of near-Chandrasekhar-mass white dwarfs (WD).

Among these new transients, a wide group of peculiar hydrogen-free SNe has recently been studied in detail (including SN 2008ha: Valenti et al. 2009; Foley et al. 2009; SN 2005E: Perets et al. 2010; SN 2002bj: Poznanski et al. 2010; SN 2010X: Kasliwal et al. 2010; SN 2005cz: Kawabata et al. 2010; PTF09dav: Sullivan et al. 2011; Kasliwal et al. 2012; SN 2010et/PTF10iuv:[1] Kasliwal et al. 2012).

SNe 2002bj and 2010X are two rapidly declining SNe (Kasliwal et al. 2010). However, beyond the fast evolution that they have in common, they differ in absolute magnitude and photospheric velocities. If the light curve is powered by ^{56}Ni decay, their fast evolution indicates a very small ejected mass (e.g. 0.16 $M_\odot$ for SN 2010X; Kasliwal et al. 2010). Accretion-induced collapse (AIC) of an O–Ne–Mg WD (Nomoto, Thielemann & Yokoi 1984; Metzger, Piro & Quataert 2009), a thermonuclear helium shell detonation on a WD (Bildsten et al. 2007) and fallback core collapse (Moriya et al. 2010) are the most common scenarios proposed to explain these two SNe.

SN 2008ha is probably the faintest hydrogen poor SN ever studied so far. Its extremely low photospheric velocity and fast light-curve evolution (but not as fast as in the rapidly declining SNe mentioned above) are consistent with a very low mass and kinetic energy (Valenti et al. 2009). Given these characteristics, the same models as mentioned above have been proposed to explain SN 2008ha. However, a few additional models have been suggested, including Fe or ONe core collapse triggered by electron captures (Pumo et al. 2009) or a failed deflagration of a carbon–oxygen WD (Foley et al. 2009). Recently, due to its spectral similarity with SN 2002cx, SN 2008ha has been included as a low-velocity and low-mass member of the SN Iax subclass (Foley et al. 2013). SNe Iax include objects with spectra similar to those of SN 2002cx, but that show a wide range of line velocities and luminosities (Foley et al. 2013). Most SNe belonging to this class exploded in late-type galaxies.

In this paper, we will mostly focus on a group of objects often referred to as 'Ca-rich transients' (Filippenko et al. 2003; Perets et al. 2010). These are faint Type I supernovae (SNe I), which reach peak absolute magnitudes of $M_R \gtrsim -16$ and exhibit photospheric expansion velocities of $\sim$11 000 km s^{-1}. They preferentially occur in the outskirts of their presumed host galaxies (Perets et al. 2010; Kasliwal et al. 2012) and their designation stems from prevalent [Ca II] lines that dominate their spectra soon after maximum.

The first recognized member of this class is SN 2005E, for which Perets et al. (2010) inferred a calcium mass of 0.135 $M_\odot$, which is much larger than ever seen in other SNe, combined with a very low total ejected mass ($\sim$0.3 $M_\odot$). Its location, the He-rich spectra, the low luminosity, and the small ejected mass led Perets et al. (2010) to suggest a helium detonation on a helium-accreting WD. Other members of this group of objects are SN 2005cz, SN 2010et and PTF11bij. They all show strong Ca lines, He lines in early spectra, weak O features in late spectra, a modest luminosity and a fast transition to the nebular phase. The latter property is a robust evidence of small ejecta mass.

The detection of strong [Ca II] lines is not a unique property of this group of SNe, since these are occasionally detected in other SN types as well. For example, faint SNe IIP also exhibit strong [Ca II] lines at late phases (Pastorello et al. 2004). Similarly, SN 2008ha shows strong [Ca II] lines. However, this SN differed from all other 'Ca-rich objects' in being very faint, evolving rapidly and having a remarkably low photospheric velocity. Since the detection of strong [Ca II] features may be common to different SN types (including objects without an enhanced Ca abundance), we will instead refer to these objects as faint SNe I, based on their observational characteristics as H-deficient SNe with $M \gtrsim -16$.

Presented in this paper are observations of the faint SN I 2012hn, acquired by the Public ESO Spectroscopic Survey for Transient Objects (PESSTO).[2] The overall science goal of PESSTO is to provide a public data base of high-quality optical + near-infrared (NIR) spectral time series of 150 optical transients covering the full parameter space that modern surveys deliver in terms of luminosity, host metallicity and explosion mechanisms. SN 2012hn is a PESSTO Key Science target as it conforms with the science goal to study unusual and unexplained transients.

The data of SN 2012hn are presented and compared with other faint SNe I: SN 2005E, SN 2005cz, SN 2010et and PTF11bij. Kasliwal et al. (2012) included also in this class PTF09dav (Sullivan et al. 2011) and SN 2007ke (Filippenko et al. 2007), and identified possible other class members in archival data.

PTF09dav is the only object within this group that spectroscopically resembles 1991bg-like SNe Ia, but with scandium and

[1] SN 2010et was discovered by Drake et al. (2010) and independently, but never announced, by the PTF (Rau et al. 2009).

[2] In response to the first call by the European Southern Observatory (ESO) for public spectroscopic surveys and particularly prompted by the opportunities provided by currently running wide-field surveys, PESSTO was awarded 90 nights yr^{-1} on the New Technology Telescope (NTT) for 4 yr, with continuation dependent on a mid-term review and the possibility for a fifth year of operations depending on the future of La Silla.

Table 1. Journal of spectroscopic observations. The spectra are available in electronic format on WISeREP (the Weizmann interactive SN data repository – Yaron & Gal-Yam 2012).

Date	JD −240 0000	Phase[a] (d)	Range (Å)	Resolution FWHM[b] (Å)	Equipment[c]
2012-04-14	560 31.52	−3	3800–9200	27	NTT+EFOSC2+Gr13
2012-04-20	560 38.54	+4	3400–10 000	15	NTT+EFOSC2+Gr11/Gr16
2012-04-22	560 40.49	+6	3400–10 000	15	NTT+EFOSC2+Gr11/Gr16
2012-04-29	560 47.50	+13	3400–10 000	15	NTT+EFOSC2+Gr11/Gr16
2012-05-11	560 59.48	+25	3000–24 000	1,2.8	VLT+XSHOOTER
2012-05-18	560 66.49	+32	3700–9000	8	MAG+LDSS3+VPH
2012-09-13	561 83.87	+149	3000–10 000	1	VLT+XSHOOTER
2012-09-14	561 84.87	+150	3000–10 000	1	VLT+XSHOOTER

[a]Relative to *R*-band maximum light (JD = 245 6034.5).
[b]Full width at half-maximum (FWHM) of night-sky emission lines.
[c]NTT: ESO New Technology Telescope; VLT: ESO Very Large Telescope; MAG: magellan.

strontium features in photospheric spectra (Sullivan et al. 2011), and weak hydrogen emission during the nebular phase (Kasliwal et al. 2012). It was initially identified as a peculiar subluminous SN Ia (Sullivan et al. 2011) and later included by Kasliwal et al. (2012) in the group of 'Ca-rich transients'. Note that scandium has never been identified in SNe whose thermonuclear origin is uncontroversial, but that it is frequently observed in SNe II (Pastorello et al. 2004) and occasionally in SNe Ib/c (e.g. SN 2007gr; Valenti et al. 2008a). SN 2007ke has been added on the basis of a strong feature at 7300 Å identified as [Ca II] λλ7291,7323 in a spectrum 19 d after maximum.

Whenever possible, PTF09dav and SN 2007ke have been included in the discussion even though their link with the other objects is less secure. The other possible members of this class, identified in archival data, are not included in this paper. The lack of quality data for most of them makes it even more difficult to establish their physical link with the group of faint SNe I. Some of the SNe Iax recently presented by Foley et al. (2013) are in principle faint SNe I (e.g. SN 2008ha), but their spectra are quite different, they explode in a different environment (Lyman et al. 2013) and they will not be discussed extensively here.

2 DATA

SN 2012hn was discovered by the CRTS on 2012 March 12.43 (UT dates are used throughout this paper) and classified at the ESO-NTT on 2012 March 14.02 as a peculiar SN Ic with some unidentified features (Benitez-Herrera et al. 2012) during an ELP[3] observing run. No objects with similar spectra were identified in the Padova Supernova archive, making SN 2012hn an interesting and rare type of SN.

Given its right ascension (see the next section), SN 2012hn could be followed only for ∼2 months after discovery. We collected four spectra with NTT+EFOSC2 (ESO Faint Object Spectrograph and Camera) in April and two spectra [with VLT+XSHOOTER and Magellan+LDSS3 (Low Dispersion Survey Spectrograph 3)] in May. Two nebular spectra were obtained with VLT+XSHOOTER on 2012 September 13.37 and 14.37. Photometry was collected mostly with NTT+EFOSC2 and the PROMPT 5 telescope (Reichart et al. 2005), with a handful of points added by the TRAPPIST and Du Pont telescopes. The log of our spectroscopic observations of SN 2012hn is reported in Table 1, and the photometry in Tables A1 and A2.

The NTT spectra were reduced using a custom-built PYTHON/PYRAF package developed by the author to reduce PESSTO data. Spectral reduction within the NTT pipeline includes corrections for bias and fringing, wavelength and flux calibration, correction for telluric absorptions and a check on the correctness of the wavelength calibration using the atmospheric emission lines. The VLT+XSHOOTER spectra were reduced using the ESO-XSHOOTER pipeline version 1.0.0 under the GASGANO framework. The Magellan+LDSS3 spectrum was reduced in a standard fashion using IRAF. Imaging data were reduced using the QUBA pipeline (see Valenti et al. 2011). The SN photometry was measured trough point spread function (PSF) fitting and calibrated against a set of local sequence stars. The latter were calibrated with respect to Landolt and Sloan standard fields during two photometric nights at the NTT. The magnitude errors account for the uncertainties in the PSF fit and the zero-points (photometric calibration). The magnitudes of the local sequence stars are reported in Tables A3 (Landolt system) and A4 (Sloan system). Our spectral sequence and light curves are shown in Fig. 1.

Already, in the first spectrum, SN 2012hn showed prominent lines that are usually observed in SNe with relatively low temperatures. The spectra are red with a drop in luminosity below 5300 Å that yields an SN $B - V$ colour ∼2. The B band evolves much faster than other optical bands, and its peak likely occurred earlier than the discovery. Whether SN 2012hn is intrinsically very red or it is red because of dust extinction along the line of sight is not obvious. Unfortunately, for this kind of transients, a robust method to estimate the extinction does not exist. For this reason, in the next section, we will discuss different reddening scenarios.

3 HOST AND REDDENING

SN 2012hn is located at $\alpha = 06^{\rm h}42^{\rm m}42\overset{\rm s}{.}55$ and $\delta = -27^{\circ}26'49\overset{''}{.}8$, 44.2 arcsec north and 18.7 arcsec east of the nucleus of NGC 2272, an E/S0-type galaxy[4] (see Fig. 2 and Table 2). Assuming a distance of 26.8 ± 1.9 Mpc for NGC 2272,[5] SN 2012hn lies at a projected distance of 6.2 kpc from the centre of the host. To compare the SN location against the host-galaxy light/stellar-mass distribution,

[3] The European Large Program was a large NTT programme (PI: S. Benetti) used to study nucleosyntesis of SNe. The project ended in 2012 September and shared time with PESSTO during period 89.

[4] Galaxy type from LEDA (Paturel et al. 2003).

[5] From NASA/IPAC Extragalactic Database (NED), including a correction for Local Group infall on to the Virgo cluster.

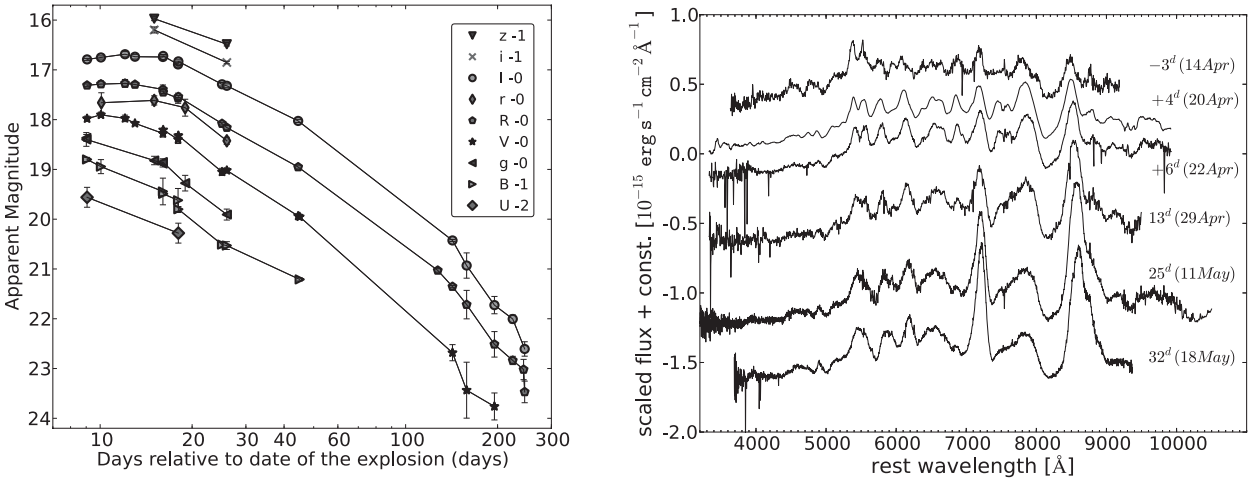

Figure 1. Left: photometry of SN 2012hn in *UBgVrRiIz*. The date of the explosion has been fixed 12 ± 3 d before *R*-band maximum light ($JD_{exp} = 245\,6022.5$). Right: full sequence of photospheric spectra collected for SN 2012hn.

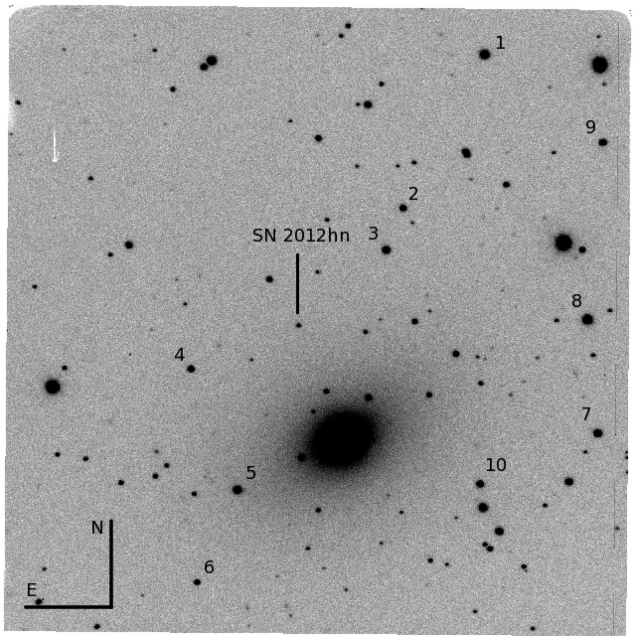

Figure 2. NTT+EFOSC2 *R*-filter image of the field of SN 2012hn (4×4 arcmin^2). The local sequence stars of Tables A3 and A4 are labelled.

Table 2. Main parameters for SN 2012hn and its host galaxy.

Parent galaxy	NGC 2272
Galaxy type	E/S0 (LEDA) / SAB0 (NED)
RA (J2000)	$06^h42^m42\overset{s}{.}55$
Dec. (J2000)	$-27°26'49\overset{''}{.}8$
Recession velocity[a]	1917 km s^{-1}
Distance modulus[b]	32.14 ± 0.15 mag
$E(B-V)_{NGC\,2272}$	0.2 mag
$E(B-V)^c_{MW}$	0.105 mag
Offset from nucleus	18.75 arcsec E, 44.20 arcsec N
Maximum epoch in *V* (JD)	$245\,6032.5 \pm 1.0$ (2012 April 15)
Maximum epoch in *R* (JD)	$245\,6034.5 \pm 1.0$ (2012 April 17)

[a]From LEDA, velocity corrected for Local Group infall on to the Virgo cluster.
[b]From NED, corrected for Local Group infall on to the Virgo cluster and assuming $H_0 = 72$ km s^{-1} Mpc^{-1}.
[c]Schlegel, Finkbeiner & Davis (1998).

we estimate the enclosed light fraction using the following method: we model the projected radial surface density profile of the host galaxy using fluxes extracted in elliptical apertures and calculate the ratio of light within the ellipse defined by the SN location and the integrated galaxy flux (Yuan et al. 2013). We find that SN 2012hn lies at a distance of more than three times the half-light ellipse. The ellipse passing through the SN encloses 88 per cent of its *R*-band light or 92 per cent of its *K*-band light (using images from the 2MASS archive). The latter is often used as a proxy for stellar mass.

SN 2012hn represents another example of a peculiar event occurring in the outer regions of an early-type host. Although it is not as distant as some others (e.g. see Kasliwal et al. 2012), the 6.2 kpc is a projected distance and the deprojected offset will likely be larger. Such an apparent preference for remote locations is different from SNe Ia and II that roughly follow the light distribution in their hosts (Förster & Schawinski 2008) and from SNe Ib/c that are more centrally concentrated in galaxies (Kelly, Kirshner & Pahre 2008; Anderson & James 2009; Leloudas et al. 2011).

The remote location of SN 2012hn in the host galaxy indirectly suggests a low extinction along the line of sight. On the other hand, the observed colours of SN 2012hn are rather extreme. Few (if any) SNe have been observed to be too red, which might therefore suggest at least some extinction. A comparison of the SED with those of objects with similar spectral features is a frequently used method to estimate the reddening. An alternative approach is based on the strength of narrow sodium lines in the spectrum.

Gas and dust are often mixed, and some authors have claimed the existence of a statistical correlation between the equivalent width (EW) of Na I D lines and the colour excess (Munari & Zwitter 1997; Turatto, Benetti & Cappellaro 2003). These results have been questioned (Poznanski et al. 2011), but very recently confirmed on the basis of an analysis of a large sample of Sloan spectra (Poznanski, Prochaska & Bloom 2012). The fact that Na I D is easily saturated makes this method inaccurate for high reddening values, while at low reddening, the spread of the relation is very high. In the XSHOOTER spectrum, the Na I D doublet is identified at a redshift of 0.0076, 150 km s^{-1} displaced to the red with respect to the systemic velocity ($z = 0.0071$) (Fig. 3). We measured EWs of 0.55 and 1.0 Å for the D2 and D1 components, respectively. D1 should have twice the intensity of D2. Convolving our XSHOOTER spectrum with a Gaussian of 15 Å (which is typical

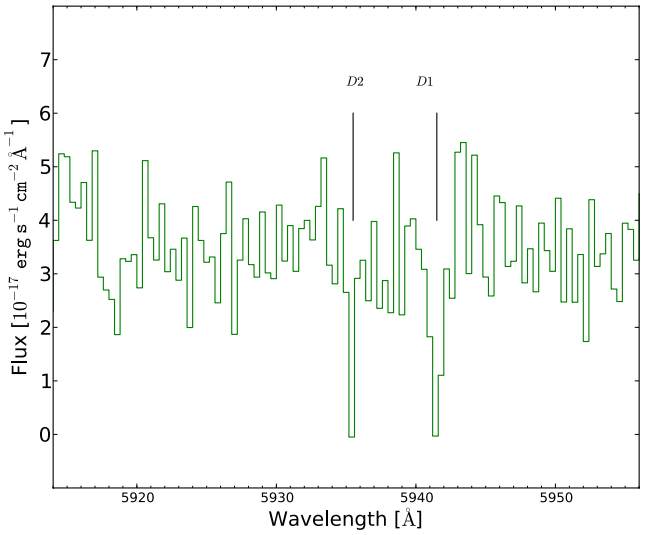

Figure 3. Na I D from the host galaxy.

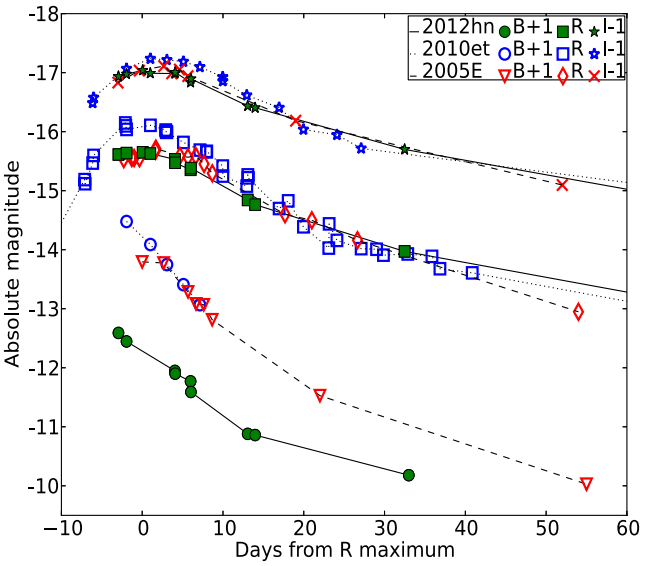

Figure 4. Light-curve comparison of SNe 2005E, 2010et and 2012hn.

of our low-resolution spectra) causes the lines to disappear, which confirms that the non-detection in the lower resolution spectra is not surprising.

Using the relation of Poznanski et al. (2012), SN 2012hn should have an $E(B-V)_{\rm NGC\,2272} = 0.2$ mag. This reddening would make SN 2012hn intrinsically very similar to the faint SNe I 2005E (Perets et al. 2010) and 2010et (Kasliwal et al. 2012) in the *R* and *I* bands, while it would remain the faintest object among these three in the *B* band (see Fig. 4). Even though a lower reddening in the host cannot be excluded, in this paper, we adopt a host-galaxy colour excess $E(B-V)_{\rm NGC\,2272} = 0.2$ mag for SN 2012hn.

4 LIGHT CURVES

Photometrically, SNe 2005E and 2010et provide the closest matches to SN 2012hn. Among the other faint SNe I, SN 2005cz (Kawabata et al. 2010) and PTF11bij (Kasliwal et al. 2012) show a similar decline in the *R* band, but due to poor coverage around maximum, the peak luminosity is not well constrained (see Fig. 5a). PTF09dav (Sullivan et al. 2011) has very similar luminosity in the *R* band, while SN 2007ke is brighter and has a broader light curve than all the other objects of this class. Its connection to the faint type I transient family cannot be safely established.

It has been claimed that 'Ca-rich' SNe show a faster luminosity evolution than other SNe I. Their light curves likely have a rise time $\leq$15 d (Kasliwal et al. 2012) and they seem to evolve faster than normal SNe Ia and most SNe Ib/c. The rise time of SNe Ia is $\sim$18 d (Hayden et al. 2010; Ganeshalingam, Li & Filippenko 2011), while on average SNe Ib have a rise time $\geq$20 d (Valenti et al. 2011). However, while SN 2010et has a similar time evolution to SN 1994I, one of the fastest evolving SNe Ic ever studied, SN 2005E and SN 2012hn have a slower light-curve evolution than SN 1994I and SN 2010et (see Fig. 5b and Table 3).

The colour-curve comparison in Fig. 6 confirms that SN 2012hn is very red, one magnitude redder than the closest matches, SNe 2005E and 2010et. All these SNe show a deficit of flux in the *B* band and a very fast evolution in the blue bands, suggesting a rapid cooling of the ejecta.

5 SPECTRA

SN 2012hn displays significant peculiarities in its spectral evolution. The deficit of flux in the *B* band is visible in all the spectra (see Fig. 1). The photospheric velocity, derived from spectral fits with SYNOW (Fisher 2000), is almost constant with phase. We determine an expansion velocity of $\sim$10 000 km s^{-1}, and the spectral lines appear even more blended at late times than at early phases (see Fig. 7). In addition, while the minima of the absorptions remain at the same positions, the peaks of selected emission features, though still blueshifted, move to redder wavelengths with time. In particular, the emission at $\sim$7195 Å (rest frame) shifts by $\sim$35 Å in one month (from 7180 Å on 2012 April 14.02 to 7215 Å on 2012 May 18.97). This line could be identified with forbidden [Ca II] λλ7291,7323. Its intensity increases with time (as expected for forbidden lines) and the blueshift goes from 5000 km s^{-1} in the first spectrum to 3500 km s^{-1} in the last photospheric spectrum, assuming that the identification with [Ca II] λλ7291,7323 is correct. Noticeably, this line is already visible in our first spectrum, taken before maximum light. The unusual velocity evolution in SN 2012hn is difficult to explain. Normally, absorption lines in SNe tend to become narrower with time, as the outer layers become more diluted by the expansion of the ejecta and the line-forming region recedes to lower velocities. In SN 2012hn, we observe the opposite trend: constant photospheric velocity (as inferred from the blueshift of absorption lines) and increasing linewidths.

5.1 Spectra of faint SNe I

In Fig. 8, we show a set of spectra that includes several faint type I objects (SNe 2005E, 2005cz and 2010et) and the peculiar PTF09dav. SNe 2005E and 2010et appear to be very similar, except for the intense peak at $\sim$4500 Å visible in SN 2005E. He I is detected in both of them and strong Ca II lines appear later on. On the other hand, there are several differences with the spectra of PTF09dav as already pointed out by Kasliwal et al. (2012). In particular, the lack of He I features and the presence of Sc II lines make PTF09dav an outlier. We note that He I is also absent in the spectra of SN 2012hn, and we do not see any evidence for the presence of Sc II lines. The spectra of SN 2012hn are also quite different from the spectra of SNe 2005E and 2010et (see Fig. 8). This implies a high degree of heterogeneity in the spectra of faint type I objects, raising the

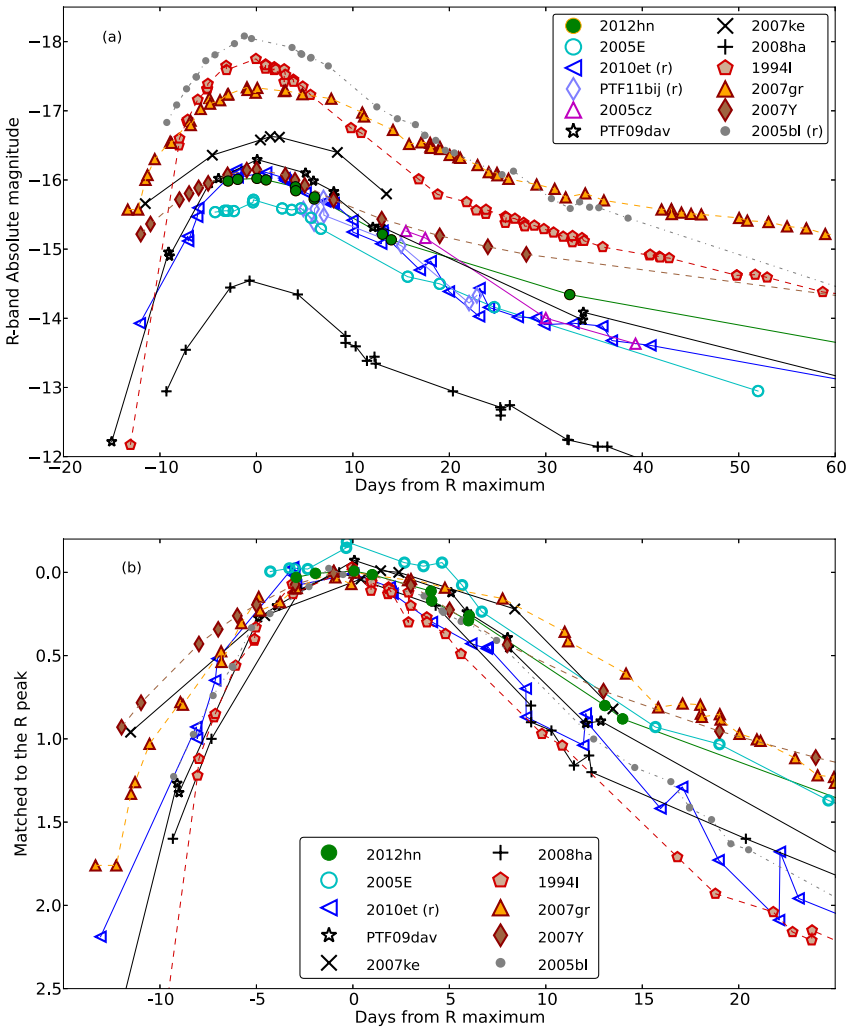

Figure 5. *R*-band photometry of SN 2012hn in comparison with other objects. Cool colours (open symbols) are used for faint SNe I that share similarities with SN 2012hn, black symbols for other faint SNe I for which the link with SN 2012hn is less secure, warm colours (filled symbols) for CC SNe. Data: SN 1994I, Richmond et al. (1996); SN 2005E, Perets et al. (2010); SN 2005bl, Taubenberger et al. (2008); SN 2005cz, Kawabata et al. (2010); SN 2007Y, Stritzinger et al. (2009); SN 2007gr, Valenti et al. (2008a) and Hunter et al. (2009); SN 2007ke, Kasliwal et al. (2012); SN 2008ha, Valenti et al. (2009); PTF09dav, Sullivan et al. (2011); SN 2010et, Kasliwal et al. (2012); PTF11bij, Kasliwal et al. (2012).

Table 3. Summary of faint type I spectrophotometric parameters.

SN	Peak magnitude *R*	Stretch factor[a]	Photospheric velocity (km s^{-1})	Hydrogen	Helium	Scandium	Oxygen	Limiting magnitude for a dwarf host
2012hn	−15.65 (33)	1.88 (20)	10 000	No	No	No	Yes	−11
2005E	−15.68 (10)	1.60 (10)	11 000	No	Yes	No	Yes	−7.5
2010et	−16.12 (12)	1.10 (10)	10 000	No	Yes	No	Yes	−12.1
PTF11bij	–	–	–	No	–	–	Yes	−12.4
2005cz	–	–	≥11 000	No	Yes	No	Yes	−7.77
2007ke	−16.62 (30)	1.72 (20)	11 000	No	Yes	No	Yes	–
PTF09dav	−16.30 (16)	1.30 (19)	6000	Yes	No	Yes	No	−9.8

[a]Stretch factor is computed using SN 1994I as reference.

possibility that not all of these objects come from the same progenitor systems or share the same explosion mechanism.

As previously mentioned, at the classification stage, we did not find objects in any of the publicly available archives with a spectrum similar to that of SN 2012hn, and we were unable to identify all the spectral lines. In principle, the lack of strong H and He I lines would favour the classification as a peculiar SN Ic. Indeed, the comparison with a library of SN spectra via GELATO (Harutyunyan et al. 2008) shows a best match with SN 1990aa (Filippenko, Shields & Petschek 1990) and several other SNe Ic.

In Fig. 9(a), we compare SN 2012hn with SN 1990aa (Matheson et al. 2001). The spectrum of SN 2012hn shows in parts the same features as SN 1990aa, although some emission features are much stronger in the former. This may however be due to the fact that

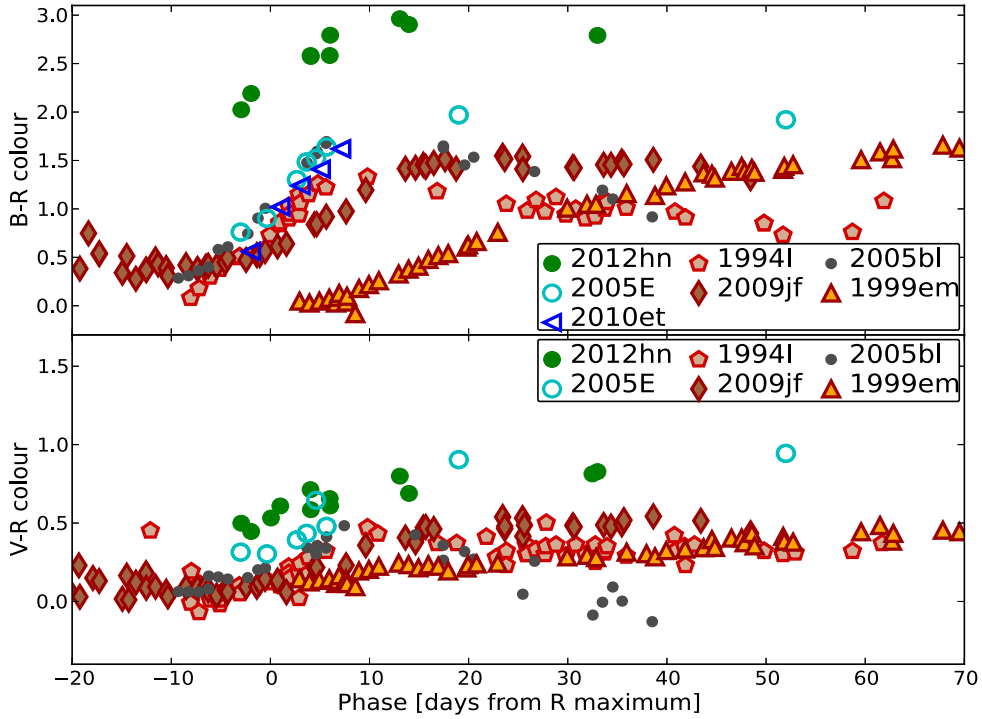

Figure 6. The $B - R$ and $V - R$ colour curves for a sample of SNe. Data: SN 1999em, Elmhamdi et al. (2003); SN 2005cf, Pastorello et al. (2007a); SN 2009jf, Valenti et al. (2011); see Fig. 5 for the references for other SNe.

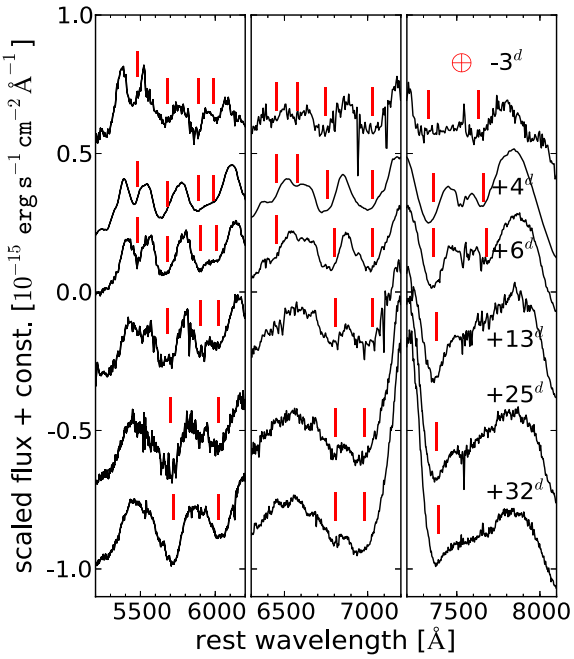

Figure 7. Detail evolution of the spectra sequence of SN 2012hn. Minima visible in the spectra have been marked at different epochs.

the spectrum of SN 2012hn is more evolved. The main differences are the strong emissions at ∼6100, ∼7200 and ∼8700 Å. Around 7500 Å, SN 1990aa shows O I λ7774, which is not visible in SN 2012hn.

In the case of SN 2005E, the most similar object was identified in SN 1990U (Perets et al. 2010). A comparison is shown in Fig. 9b. Both SN 2005E and SN 1990U show He I λ5876, λ7065 lines. In the spectrum of SN 1990U, He I λ6678 is detected, although contaminated by narrow Hα from the host galaxy, while it is weak or absent in the spectrum of SN 2005E.

It is interesting to point out that both SN 2012hn and SN 2005E are similar to quite normal SNe Ic and SNe Ib, respectively, though with more prominent Ca features. Given these similarities, it is tempting to propose that faint SNe I might arise from similar progenitors as SNe Ib/c, though with an overproduction of Ca in the explosive nucleosynthesis or with ionization and excitation conditions in the ejecta that favour the formation of strong Ca II features.

Starting from the similarity with SN 1990aa, we used SYNOW to identify the lines in the SN 2012hn spectra. Fits to the spectra collected on April 20 (+4 d) and May 18 (+32 d) are shown in Figs 10a and 10b, respectively. A photospheric velocity of 10 000 km s^{-1} was adopted in both cases, while we used temperatures of 4500 K for the spectrum at +6 d and 4200 K for the spectrum at +32 d. The radial dependence of the line optical depths was chosen to be exponential with the e-folding velocity v_e [i.e. $\tau \propto \exp(-v/v_e)$] set to 1000 km s^{-1} for both spectra. The spectra can be reproduced reasonably well with a small number of ions, including Fe II, Ca II, C I, Cr II, Ti II and Na I. Most lines between 6000 and 7500 Å can be reproduced by enhancing Fe II and Ti II. The line at ∼5800 Å may be reproduced by Na I and Cr II or detached He I, but we consider the He I identification unlikely because of the lack of other He I lines both in the optical and the NIR regime (see Section 5.2). Some Fe II lines may also contribute to this feature. Between 7200 and 7800 Å, SN 2012hn shows two absorption features, redwards and bluewards, respectively, of the expected position of O I λ7774. Mg II is an alternative for the absorption at 7700 Å, redwards of the usual O I position. The absorption at ∼7350 Å, bluewards of the usual O I position, may still be explained with O I. We stress that Si II is not required to reproduce the spectrum (see the inset of Fig. 10a), while some S II might possibly contribute to the absorption at ∼5500 Å.

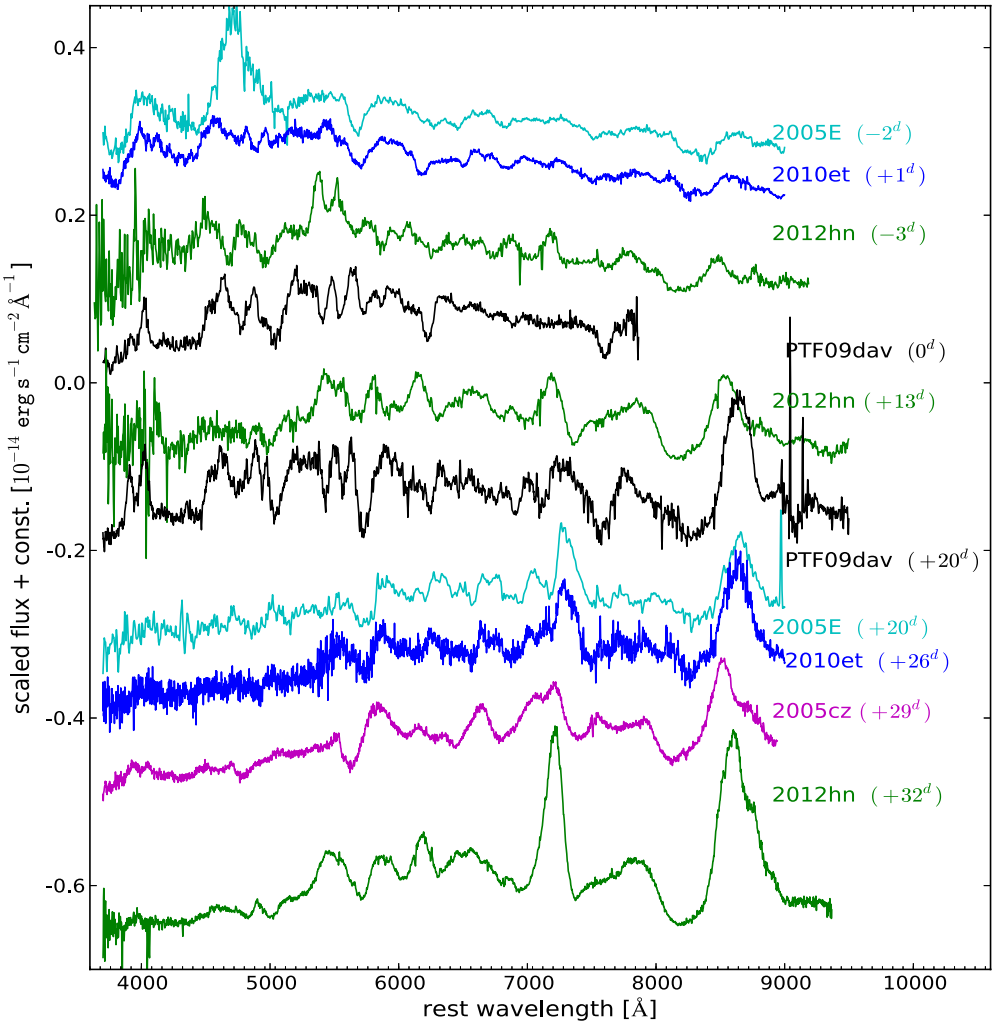

Figure 8. Spectra comparison of SNe that have been suggested as 'Ca rich'. See Fig. 5 for references.

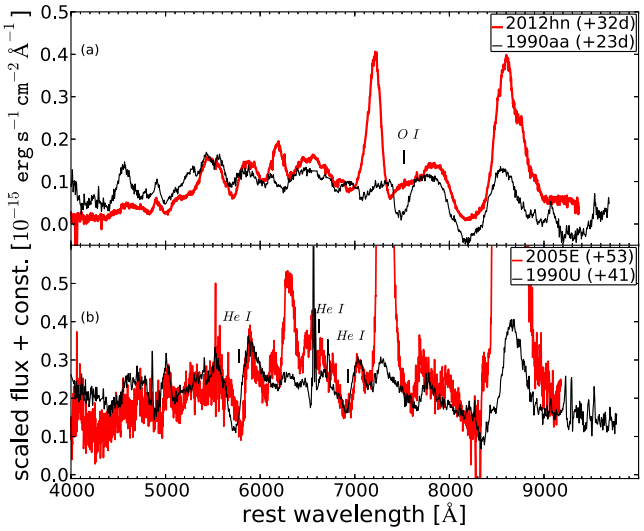

Figure 9. Comparison of SN 2012hn and SN 2005E with SN 1990aa and SN 1990U, respectively. The latter have been identified as best spectroscopic matches to the former. Data are from Matheson et al. (2001) and Filippenko (1992).

In the first spectrum including some Ba II may help to reproduce the feature at 5900 Å. The presence of Ba II, if confirmed, would be important, since Ba II is not expected in thermonuclear explosions. Unfortunately, we consider this identification not as secure as other identifications, since it is mainly based on a single line.

The main shortcomings of the synthetic spectrum are the emission features at ∼7200 and ∼8700 Å which are not reproduced. If the former (∼7200 Å) is identified as blueshifted [Ca II] or [O II], the poor fit is not surprising, since SYNOW cannot reproduce forbidden lines.

5.2 SN 2012hn NIR spectrum

The XSHOOTER spectrum of SN 2012hn collected on 2012 May 11.98 for the first time gives us the possibility to probe the NIR spectrum of a faint SN I (see Fig. 11). The red part of the spectrum is quite noisy, but still it can be used to exclude the presence of a strong He feature at ∼2 μm, which is typical of He-rich SNe. Normal SNe Ia show intense lines of Co II and Fe II at this phase (Marion et al. 2009; Gall et al. 2012). These lines are not clearly identified in SN 2012hn. However, this is not unexpected, since the low luminosity of SN 2012hn suggests that a small amount of ^{56}Ni was synthesized in the explosion. The XSHOOTER spectrum

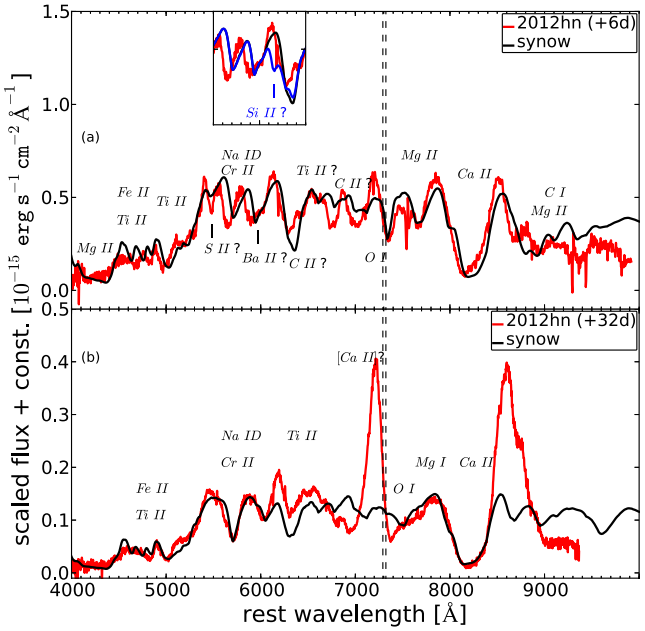

Figure 10. SYNOW fit of SN 2012hn spectra. The dashed lines indicate the rest-frame positions of [Ca II] λλ7291,7323. The inset in the upper panel shows that adding Si II (blue line) deteriorates the SYNOW fit to the observed spectrum.

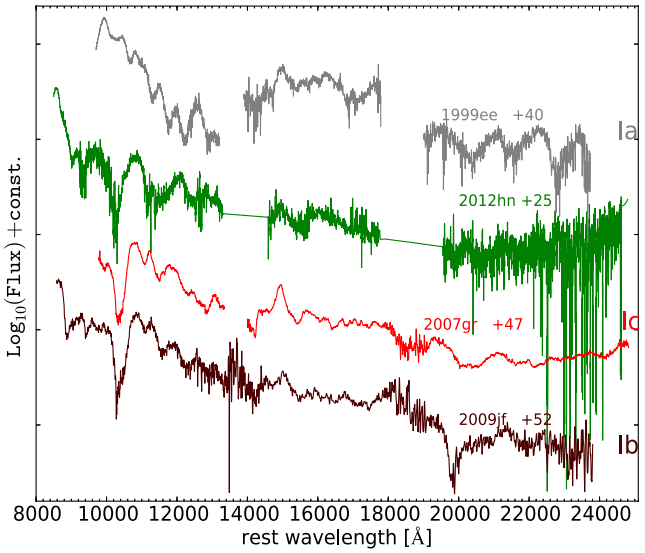

Figure 11. XSHOOTER NIR spectrum of SN 2012hn in comparison with spectra of other SNe. The SN 2012hn spectrum has been rebinned to 20 Å bins. Comparison spectra are from Hamuy et al. (2002); Hunter et al. (2009); Sahu et al. (2011).

also gives us information on the amount of flux emitted in the NIR. After checking the XSHOOTER spectrum flux calibration with our optical photometry, we computed a synthetic $R-H$ colour ($\sim -0.5 - 0.0$ mag). This value is comparable with the $R-H$ colour of several SNe Ia (Krisciunas et al. 2004) and much lower than the $R-H$ colour of core-collapse SNe at this phase ($R-H \sim 1$ mag).

5.3 Late-time spectroscopy

Two XSHOOTER spectra were obtained 149 and 150 d after R-band maximum, and the combination of their optical parts is compared with nebular spectra of different types of SNe in Fig. 12. No flux has been detected in the NIR part of the combined XSHOOTER spectrum down to a magnitude of ∼22.5 in the H band.

The emission centred at ∼7250 Å is most likely [Ca II] λλ7291,7323, with a contribution of [Fe II] to the blue (λλ7155,7172) and the red (λλ7388,7452) wings. Mg I] λ4571 is also detected. No permitted lines of O I (λ7774 or λ8446) are visible, and also the Ca NIR triplet, very strong at early phases, has faded. An emission feature at ∼8700 Å is likely a blend of residual, weak Ca II and [C I] λ8727. The absence of permitted lines gives us a constraint on the density, confirming that the spectrum is nebular (Fransson & Chevalier 1989). Comparing SN 2012hn with other faint SNe I, the weakness of the Ca II NIR triplet is not unusual. However, the prominent [O I] λλ6300,6364 feature is quite unique among faint SNe I. It is much more similar in terms of relative strength to spectra of stripped core-collapse SNe, which show strong [O I] owing to oxygen produced in the progenitor star. The feature is symmetric around the rest wavelength and relatively narrow, with emission out to 3500 km s^{-1}. No narrow lines from the host galaxy are visible in the spectrum. Using equation 2 from Kennicutt (1998) and an Hα upper limit of 3×10^{-18} erg s^{-1} cm^{-2}, we obtained an upper limit for the star formation rate of 2×10^{-6} M$_\odot$ yr^{-1}.

We computed the [Ca II]/[O I] ratio for a large set of nebular spectra of core-collapse SNe and the sample of faint SNe I presented by Kasliwal et al. (2012) (see Fig. 13). For almost all core-collapse SNe, [Ca II] λλ7291,7323 starts to be visible earlier than [O I] λλ6300,6364, but rarely less than 100 d after maximum light. Faint SNe I show both these lines earlier on, but no data are available later than 170 d after maximum to study the intensity evolution of these features over longer time-scales. Fig. 13 confirms that at 150 d after maximum, the [Ca II]/[O I] ratio of SN 2012hn is at the edge of the region occupied by core-collapse SNe.

6 BOLOMETRIC LIGHT CURVE

To constrain the physical parameters of SN 2012hn ($M_{\rm Ni}$, $M_{\rm ej}$ and $E_{\rm k}$), we computed a pseudo-bolometric light curve using the available photometric information. As long as the light curve is powered by the ^{56}Ni → ^{56}Co → ^{56}Fe decay chain, a brighter bolometric light curve implies a larger amount of ejected ^{56}Ni. In addition, the broader the light curve, the higher is the ejected mass and/or the lower the kinetic energy released in the explosion (Arnett 1982).

To compute the pseudo-bolometric light curve, the observed magnitudes were corrected for reddening [$E(B-V)_{\rm NGC\,2272} = 0.2$ mag], converted to flux densities at the effective wavelengths and integrated using Simpsons rule. The so-created pseudo-bolometric light curve is plotted in Fig. 14 together with those of other SNe computed following the same prescriptions. In core-collapse SNe, the NIR flux contributes up to 40–50 per cent to the total flux and in SNe Ia up to 30 per cent (Valenti et al. 2008b). Given the $R-H$ colour measured from our first XSHOOTER spectrum, we assumed that the fractional contributions of the UV and NIR emission to the bolometric light curve of SN 2012hn are the same as for the SN Ia 2005cf (Pastorello et al. 2007a). With this assumption, we computed a *uvoir* pseudo-bolometric light curve of SN 2012hn, which is also shown in Fig. 14.

The lack of data before maximum and hence the unknown rise time of SN 2012hn makes it difficult to derive accurate explosion parameters. A rough estimate of $M_{\rm ej}$ and $E_{\rm k}$ can be computed guided by the comparison with well-studied SNe and the following simple relations: $v \propto (E_{\rm k}/M_{\rm ej})^{1/2}$ and $t_{\rm s} \propto (M_{\rm ej}^3/E_{\rm k})^{1/4}$, where v is the photospheric velocity (evaluated at maximum light) and $t_{\rm s}$ is the time-scale of the photospheric phase (Arnett 1982).

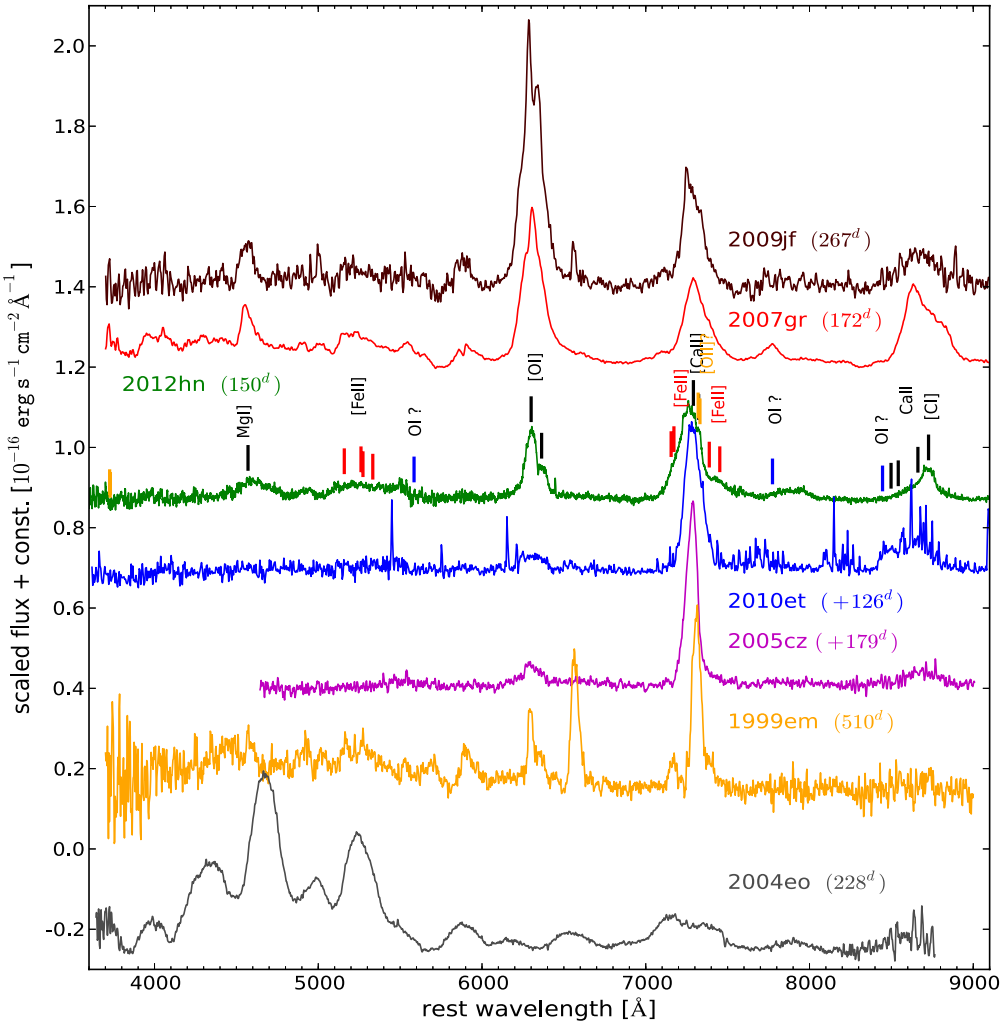

Figure 12. Nebular spectrum of SN 2012hn in comparison with a set of nebular spectra of different types of SNe. Tentative line identifications are given for the spectrum of SN 2012hn. Data: SN 2009jf, Valenti et al. (2011); SN 2007gr, Hunter et al. (2009); SN 2010et, Kasliwal et al. (2012); SN 2005cz, Kawabata et al. (2010); SN 1999em, Elmhamdi et al. (2003); SN 2004eo, Pastorello et al. (2007b).

Using a Chandrasekhar-mass SN Ia as comparison ($E_k = 1.3 \times 10^{51}$ erg, $M_{ej} = 1.4\,M_\odot$, $v = 10\,000\,km\,s^{-1}$), the photospheric velocity of SN 2012hn ($v = 10\,000\,km\,s^{-1}$) and a time-scale of t_s(SN2012hn) = 0.7–0.8 t_s(SNeIa) (from light-curve comparisons), we obtain the following values for SN 2012hn: $M_{ej} = 0.7$–$0.9\,M_\odot$ and $E_k = 0.65$–0.85×10^{51} erg. Using instead the SN Ic 2007gr as reference, adopting the values of M_{ej} and E_k reported by Hunter et al. (2009), we obtain the following estimate for the energy and the ejected mass: $M_{ej} = 1.2$–$2.1\,M_\odot$ and $E_k = 0.74$–3×10^{51} erg.

Perets et al. (2010), using the same approach, obtained much smaller values for SN 2005E ($M_{ej} = 0.25$–$0.41\,M_\odot$ and E_k =0.44–0.72×10^{51} erg). Some of the difference may come from the presence of helium in SN 2005E. As reported by Perets et al. (2010), helium is less opaque than other elements, and this may lead to an underestimate of the helium mass. But the different values obtained mainly reflect the uncertainties in some of the important fitting constraints, such as the rise time. Perets et al. (2010) indeed adopted a very short rise time of 7–9 d.

We suggest that from the light-curve comparison with SN 1994I (with a rise time of 12 d; Iwamoto et al. 1994, see the inset plot in Fig. 14), a rise time of 7–9 d for SN 2005E is probably an underestimate, unless the light curve of SN 2005E was strongly asymmetric. Using a larger rise time for SN 2005E would give ejected mass and kinetic energy larger than previously reported, more consistent with those we obtain for SN 2012hn. However, a spectral model for a not completely nebular spectrum of SN 2005E was presented by Perets et al. (2010), supporting a low ejected mass and kinetic energy for SN 2005E. Future observations of faint SNe I are needed to confirm or disprove the very small ejected masses and kinetic energies proposed for some faint SNe I.

From the absolute luminosity of SN 2012hn, if the light curve is powered by nickel decay, assuming a rise time between 10 and 15 d, the mass of ^{56}Ni produced in the explosion should be in the range $M_{Ni} = 0.005$–$0.010\,M_\odot$, where $0.005\,M_\odot$ is the lower limit considering no infrared contribution to the bolometric light curve. Assuming that the fractional contribution of the UV and NIR emission to the bolometric light curve is 40–50 per cent, a value typical for core-collapse SNe, we can fix an upper limit for the nickel produced in the explosion of $0.013\,M_\odot$.

However, as pointed out by several authors, in low-density explosions, decays of radioactive nuclei other than ^{56}Ni may be important (Shen et al. 2010; Waldman et al. 2011; Sim et al. 2012). In particular, the decays ^{48}Cr → ^{48}V → ^{48}Ti and ^{44}Ti → ^{44}Sc → ^{44}Ca may play an important role in powering the light curve. While at

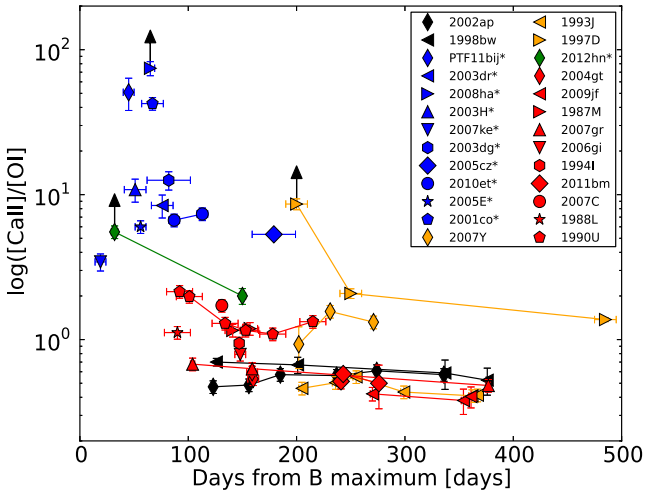

Figure 13. The [Ca II]/[O I] ratio as a function of time for a sample of SNe: stripped-envelope CC SNe (in red), broad-line stripped-envelope CC SNe (in black), He/H-rich CC SNe (in yellow), SN 2012hn (in green) and other faint SNe I (in blue). For objects labelled with '∗', the phase is given relative to *R*-band maximum or relative to discovery. Data from Taubenberger et al. (2009, and references therein), Valenti et al. (2009, 2011, 2012), Hunter et al. (2009), Stritzinger et al. (2009), Kasliwal et al. (2012), Turatto et al. (1998).

early phases, it is tricky to identify the radioactive nuclei that contribute to power the light curve, the slope of the light curve at later phases provides more information. In the former case, the slope of the light curve would be comparable or even steeper (in case of incomplete trapping of the energy) to the slope of the ^{48}V decay (half lifetime = 15.97 d), while in the latter case, the ^{44}Ti decay (half lifetime = 63 yr) would determine the observed light-curve slope. From the inferred slope of the bolometric light curve of SN 2012hn, we consider a major contribution from these alternative radioactive nuclei to the light curve unlikely.

The nickel mass produced may hence be even lower than the one reported. Ti and Cr may also be responsible for the fast evolution in the blue bands and the relatively red colour by depressing most of the flux in the blue part of the spectrum. The slope of the bolometric light curve in the tail phase is comparable to that of the SN Ia 1991bg and faster than in most other SNe. SN 2010et, the only 'Ca-rich' SN with multiband late-time photometry, shows a similar slope until 80 d after *R*-band maximum. After this point, the bolometric light curve of SN 2010et is contaminated by the flux from its host galaxy (Kasliwal et al. 2012). The steady slope of the tail of SN 2012hn suggests that a single decay is powering the light curve at these phases.

7 DISCUSSION AND CONCLUSIONS

SN 2012hn belongs to the class of faint SNe I, showing a light curve that is very similar to those of SNe 2005E and 2010et. It has a low peak luminosity and evolves rapidly (although not as fast as SN 1994I). Faint type I transients show heterogeneous spectral properties. In particular, SN 2012hn shows no clear evidence of He I features, and the early-time spectra resemble those of an SN Ic with superimposed forbidden lines of Ca II. Contrary to what we typically see in SNe, linewidths tend to increase with

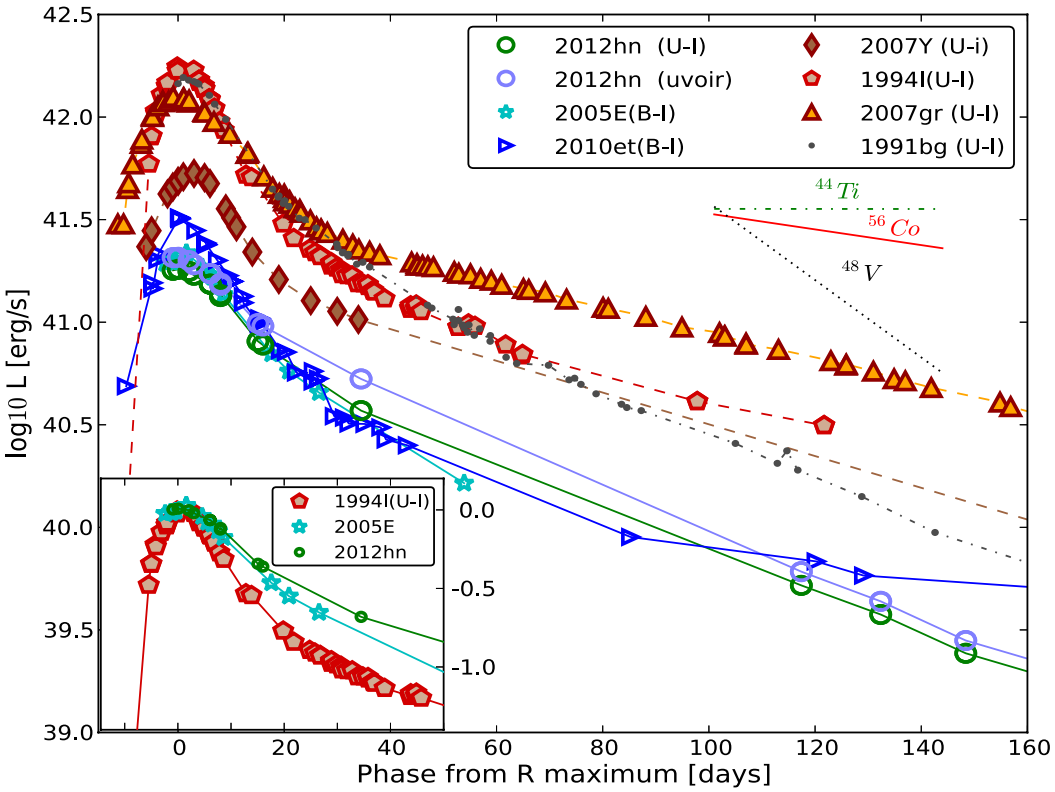

Figure 14. Pseudo-bolometric light curve of SN 2012hn in comparison with other SNe. Data: see references in Fig. 5; SN1991bg, Turatto et al. (1996). Distances and colour excesses: SN 1994I: $E(B-V) = 0.04$ mag, $\mu = 29.60$ mag, (Sauer et al. 2006); SN 2007gr: $E(B-V) = 0.092$ mag, $\mu = 29.84$ mag, (Valenti et al. 2008a); SN 2007Y: $E(B-V) = 0.112$ mag, $\mu = 31.13$ mag, (Stritzinger et al. 2009); SN 2005E: $E(B-V) = 0.041$ mag, $\mu = 32.66$ mag, (Perets et al. 2010); SN 2010et: $E(B-V) = 0.046$ mag, $\mu = 35.05$ mag, (Kasliwal et al. 2012); SN 1991bg: $E(B-V) = 0.029$ mag, $\mu = 31.44$ mag, (Turatto et al. 1996). Inset plot: pseudo-bolometric light curves of SNe 2012hn, 2005E and 1994 normalized to the maximum luminosity.

time, while the photospheric velocity remains almost constant at $\sim$10 000 km s^{-1} during the entire photospheric phase.

One of the most intriguing features is the presence, very early on, of a strong emission feature at about 7200 Å. Based on the very strong Ca II NIR triplet and the lack of viable alternatives, we attribute this feature to forbidden Ca II. However, if this is correct, the peak of the emission is blueshifted by 3000–5000 km s^{-1} with respect to the rest-frame position. Since the blueshift decreases with time, it is unlikely due to dust forming and may be explained by an optically thick core of the ejecta (Taubenberger et al. 2009) or by strong asymmetry in the explosion. On the other hand, the [O I] profile in the nebular spectrum is consistent with a spherically symmetric distribution of the ejecta, or at least of the oxygen-rich material.

In the last few years, several studies have been carried out to explain faint type I transients. Most of them have focused on He-shell detonations on accreting carbon–oxygen WDs (Bildsten et al. 2007; Shen et al. 2010; Waldman et al. 2011; Sim et al. 2012).

In the double-detonation scenario for SNe Ia, the He-shell detonation is followed by a second detonation in the core of the carbon–oxygen WD. While it is still not clear if and where the second detonation occurs (but see Fink, Hillebrandt & Röpke 2007; Kromer et al. 2010), a pure He-shell detonation might produce an explosion with several characteristics similar to the explosion of SN 2012hn. Shen et al. (2010) investigated He-shell detonations for three different WD masses (0.6, 1.0 and 1.2 $M_\odot$) and different He-shell masses (0.02, 0.05, 0.1, 0.2 and 0.3 $M_\odot$). Waldman et al. (2011) focused their study on low-mass WDs (0.45–0.6 $M_\odot$) with a 0.2 $M_\odot$ He shell. Also Sim et al. (2012) studied He-shell detonations on low-mass WDs (0.45–0.58 $M_\odot$) with a 0.21 $M_\odot$ He shell, but extended the simulations to cases where a second detonation occurs. These studies tend to find that the amount of intermediate-mass elements (Si and S) produced during the explosion is lower than in *normal* SNe Ia, whereas Ti and Cr are produced abundantly. The resultant spectrum is also rich of Ti and Cr lines. While this is consistent with the spectra of SN 2012hn, the light curve may be different. If the second detonation occurs, the models show light curves brighter than that of SN 2012hn (Sim et al. 2012). If the second detonation does not occur, the peak luminosity is comparable, but the evolution is much faster than that of SN 2012hn. Waldman et al. (2011) were able to obtain a light curve comparable to SN 2005E for their He-shell detonation model WD (0.45 $M_\odot$) +He-shell (0.2 $M_\odot$), but only with an artificial ^{44}Ti enhancement by a factor of 50. All the He-shell detonation models in low-mass WDs predict red spectra with Ti lines and no intermediate-mass elements, but none of them predict the slow spectral evolution of SN 2012hn. So far, no synthetic nebular spectra of He detonations on accreting WDs have been made. Unburned C/O can be present in an He-shell detonation if the second detonation in the WD does not occur. The He-shell detonation model of Sim et al. (2012) shows oxygen velocity below 4000 km s^{-1}, consistent with the oxygen velocity in the nebular spectrum of SN 2012hn. Whether this amount of oxygen is enough, and the density and ionization in the innermost ejecta are suited to produce the observed nebular oxygen line of SN 2012hn is still not clear. An estimate of the ejected mass of oxygen and carbon from the nebular SN 2012hn spectrum would be the next step in this analysis (Mazzali et al. 2007, 2010).

Little Si and S, the presence of Ti and Cr, and [O I] in the nebular spectrum are also expected in core-collapse SNe. Nevertheless, only few theoretical studies have been made so far to explain faint SNe I as core-collapse explosions. Kawabata et al. (2010) proposed for SN 2005cz, a progenitor of 8–12 $M_\odot$ that lost its envelope through interaction in a binary system. These stars are more abundant than more massive stars, and some of them should still be present in E/S0 galaxies. If the hydrogen layer has been stripped by a companion star, they might still produce core-collapse SNe similar to SNe Ib and Ic. As stripped-envelope counterparts of faint SNe IIP (Pastorello et al. 2004), a population of faint SNe Ib/c may be expected to exist. These objects have not been unambiguously identified in observations so far (but see Valenti et al. 2009), but faint SNe I could be viable candidates. The weak point of this interpretation is that, so far, no faint SNe IIP have been discovered in remote locations of E/S0 galaxies. Only few models for faint stripped-envelope core-collapse SNe are available. Fryer et al. (2009) presented first radiation-hydrodynamics calculations of several models for faint SNe including fallback SNe and AIC SNe. Their conclusion was that both AIC and failed thermonuclear SNe can potentially reproduce the observed light curves of faint Type I SNe, but that further studies are recommended.

In summary, the physical origin of this faint Type I SN 2012hn is still ambiguous. The location of the transient, in the remote outskirts of an E/S0-type galaxy indicates an origin in an old stellar population and hence an accreting WD system as the most likely progenitor. The lack of any possible dwarf host galaxy to quite faint magnitudes in pre-discovery images (to below about $M = -11$) argues either for a non-star-forming population or an ultrafaint dwarf galaxy with presumably low metallicity. However, the nebular spectrum of SN 2012hn at +150d shows the strongest oxygen feature yet detected among faint SNe I, similar in strength to [O I] seen in core-collapse SNe. This is not necessarily surprising, since the nebular spectrum of SN 2012hn is among most evolved and it is well known that the [O I] feature becomes more intense with time. This could also mean that the high [Ca II]/[O I] ratio seen in some faint SNe I at relative early phase may in part be a phase-dependent effect rather than reflecting an intrinsic abundance pattern. Mg I and C I features are also detected in SN 2012hn, which are weak or absent in other faint SNe I, but usually seen in core-collapse events.

Among the other faint SNe I discovered so far, SNe 2010et and 2005E have similar light curves and are in even more remote locations with respect to their hosts. This appears to be a strong argument in favour of the WD as progenitors. However, if a single scenario gives rise to these events, it must be able to reproduce the differences in their spectra, in particular the small amount of helium (if any) in SN 2012hn and the differences already mentioned in the nebular spectra, and to produce an ejected mass in the range ($\sim$0.5–1.5 $M_\odot$), comparable with the ejected masses of low-mass, low-energy SNe Ib/c. Detailed modelling of the nebular spectra of this class may help to further constrain the origins of these peculiar and intriguing explosions (e.g. Mazzali et al. 2010, 2011; Maurer et al. 2011; Jerkstrand et al. 2012) and to confirm or disprove the large Ca abundance reported for SN 2005E by Perets et al. (2010).

Including other faint transients, such as PTF09dav or SN 2008ha, in the same scenario will be even more complicated, emphasizing the possibility that faint SNe I may actually arise from several different explosion channels.

ACKNOWLEDGEMENTS

GP acknowledges support by the Proyecto FONDECYT 11090421. JA acknowledges support by CONICYT through FONDECYT grant 3110142. GP and JA acknowledge support by the Millennium Center for Supernova Science (P10-064-F), with input from Fondo de Innovacion para la Competitividad, del Ministerio de Economia, Fomento y Turismo de Chile. ST acknowledges support

by the TRR 33 'The Dark Universe' of the German Research Foundation. MS acknowledges support from the Royal Society. This work was supported by the National Science Foundation under grants PHY 11-25915 and AST 11-09174. Research leading to these results has received funding from the European Research Council under the European Union's Seventh Framework Programme (FP7/2007-2013)/ERC grant agreement no. [291222] (PI: S. J. Smartt). AP., SB and EC are partially supported by the PRIN-INAF 2011 with the project 'Transient Universe: from ESO Large to PESSTO'. Research by AGY and his group is supported by the FP7/ERC, Minerva and GIF grants. Parts of this research were conducted by the Australian Research Council Centre of Excellence for All-sky Astrophysics (CAASTRO), through project number CE110001020. We are grateful to Douglas Leonard who provided us his spectrum of SN 2005cz.

This paper is based on observations made with the following facilities: ESO Telescopes at the La Silla and Paranal Observatories under programme IDs 184.D-1140, 188.D-3003 and 089.D-0270, PROMPT Telescopes (Chile), TRAPPIST Telescope (Chile), Du Pont telescope (Chile) and Magellan telescope (Chile). Observations under programme ID 188.D-3003 are part of PESSTO (the Public ESO Spectroscopic Survey for Transient Objects). The spectra of Kasliwal et al. (2012) were downloaded from WISeREP (Yaron & Gal-Yam 2012).

REFERENCES

Anderson J. P., James P. A., 2009, MNRAS, 399, 559
Arnett W. D., 1982, ApJ, 253, 785
Benitez-Herrera S., Taubenberger S., Valenti S., Benetti S., Pastorello A., 2012, Astron. Telegram, 4047, 1
Bildsten L., Shen K. J., Weinberg N. N., Nelemans G., 2007, ApJ, 662, L95
Drake A. J. et al., 2009, ApJ, 696, 870
Drake A. J. et al., 2010, CBET, 2339, 1
Elmhamdi A. et al., 2003, MNRAS, 338, 939
Filippenko A. V., 1992, ApJ, 384, L37
Filippenko A. V., Shields J. C., Petschek A. G., 1990, IAU Circ., 5111, 1
Filippenko A. V., Chornock R., Swift B., Modjaz M., Simcoe R., Rauch M., 2003, IAU Circ., 8159, 2
Filippenko A. V., Silverman J. M., Foley R. J., Modjaz M., Papovich C., Willmer C. N. A., Blondin S., Brown W., 2007, CBET, 1101, 1
Fink M., Hillebrandt W., Röpke F. K., 2007, A&A, 476, 1133
Fisher A. K., 2000, PhD thesis, Univ. Oklahoma
Foley R. J. et al., 2009, AJ, 138, 376
Foley R. J. et al., 2013, ApJ, 767, 57
Förster F., Schawinski K., 2008, MNRAS, 388, L74
Fransson C., Chevalier R. A., 1989, ApJ, 343, 323
Fryer C. L. et al., 2009, ApJ, 707, 193
Gall E. E. E., Taubenberger S., Kromer M., Sim S. A., Benetti S., Blanc G., Elias-Rosa N., Hillebrandt W., 2012, MNRAS, 427, 994
Ganeshalingam M., Li W., Filippenko A. V., 2011, MNRAS, 416, 2607
Hamuy M. et al., 2002, AJ, 124, 417
Harutyunyan A. H. et al., 2008, A&A, 488, 383
Hayden B. T. et al., 2010, ApJ, 712, 350
Hunter D. J. et al., 2009, A&A, 508, 371
Iwamoto K., Nomoto K., Hoflich P., Yamaoka H., Kumagai S., Shigeyama T., 1994, ApJ, 437, L115
Jerkstrand A., Fransson C., Maguire K., Smartt S., Ergon M., Spyromilio J., 2012, A&A, 546, 28
Kaiser N. et al., 2002, in Tyson J. A., Wolff S., eds, Proc. SPIE , Vol. 4836, Survey and Other Telescope Technologies and Discoveries. SPIE, Bellingham, p. 154
Kasliwal M. M. et al., 2010, ApJ, 723, L98
Kasliwal M. M. et al., 2012, ApJ, 755, 161
Kawabata K. S. et al., 2010, Nat, 465, 326
Kelly P. L., Kirshner R. P., Pahre M., 2008, ApJ, 687, 1201
Kennicutt R. C., 1998, ApJ, 498, 541
Krisciunas K. et al., 2004, AJ, 128, 3034
Kromer M., Sim S. A., Fink M., Röpke F. K., Seitenzahl I. R., Hillebrandt W., 2010, A&A, 514, A53
Leloudas G. et al., 2011, A&A, 530, 95
Lyman J. D., James P. A., Perets H. B., Anderson J. P., Gal-Yam A., Mazzali P., Percival S. M., 2013, MNRAS, 434, 537
Marion G. H., Höflich P., Gerardy C. L., Vacca W. D., Wheeler J. C., Robinson E. L., 2009, AJ, 138, 727
Matheson T., Filippenko A. V., Li W., Leonard D. C., Shields J. C., 2001, AJ, 121, 1648
Maurer I., Jerkstrand A., Mazzali P. A., Taubenberger S., Hachinger S., Kromer M., Sim S., Hillebrandt W., 2011, MNRAS, 418, 1517
Mazzali P. A. et al., 2007, ApJ, 670, 592
Mazzali P. A., Maurer I., Valenti S., Kotak R., Hunter D., 2010, MNRAS, 408, 87
Mazzali P. A., Maurer I., Stritzinger M., Taubenberger S., Benetti S., Hachinger S., 2011, MNRAS, 416, 881
Metzger B. D., Piro A. L., Quataert E., 2009, MNRAS, 396, 1659
Moriya T., Tominaga N., Tanaka M., Nomoto K., Sauer D. N., Mazzali P. A., Maeda K., Suzuki T., 2010, ApJ, 719, 1445
Munari U., Zwitter T., 1997, A&A, 318, 269
Nomoto K., Thielemann F.-K., Yokoi K., 1984, ApJ, 286, 644
Pastorello A. et al., 2004, MNRAS, 347, 74
Pastorello A. et al., 2007a, MNRAS, 376, 1301
Pastorello A. et al., 2007b, MNRAS, 377, 1531
Paturel G., Petit C., Prugniel Ph., Theureau G., Rousseau J., Brouty M., Dubois P., Cambrésy L., 2003, A&A, 412, 45
Perets H. B. et al., 2010, Nat, 465, 322
Poznanski D. et al., 2010, Sci, 327, 58
Poznanski D., Ganeshalingam M., Silverman J. M., Filippenko A. V., 2011, MNRAS, 415, L81
Poznanski D., Prochaska J. X., Bloom J. S., 2012, MNRAS, 426, 1465
Pumo M. L. et al., 2009, ApJ, 705, L138
Quimby R. M., 2006, PhD thesis, Univ. Texas
Rau A. et al., 2009, PASP, 121, 1334
Reichart D. et al., 2005, Nuovo Cimento C, 28, 767
Richmond M. W. et al., 1996, AJ, 111, 327
Sahu D. K., Gurugubelli U. K., Anupama G. C., Nomoto K., 2011, MNRAS, 413, 2583
Sauer D. N., Mazzali P. A., Deng J., Valenti S., Nomoto K., Filippenko A. V., 2006, MNRAS, 369, 1939
Schlegel D. J., Finkbeiner D. P., Davis M., 1998, ApJ, 500, 525
Shen K. J., Kasen D., Weinberg N. N., Bildsten L., Scannapieco E., 2010, ApJ, 715, 767
Sim S. A., Fink M., Kromer M., Röpke F. K., Ruiter A. J., Hillebrandt W., 2012, MNRAS, 420, 3003
Stritzinger M. et al., 2009, ApJ, 696, 713
Sullivan M. et al., 2011, ApJ, 732, 118
Taubenberger S. et al., 2008, MNRAS, 385, 75
Taubenberger S. et al., 2009, MNRAS, 397, 677
Turatto M., Benetti S., Cappellaro E., Danziger I. J., Della Valle M., Gouiffes C., Mazzali P. A., Patat F., 1996, MNRAS, 283, 1
Turatto M. et al., 1998, ApJ, 498, L129
Turatto M., Benetti S., Cappellaro E., 2003, in Hillebrandt W., Leibundgut B., eds, Proc. ESO/MPA/MPE, From Twilight to Highlight: The Physics of Supernovae. Springer-Verlag, Berlin, p. 200
Valenti S. et al., 2008a, ApJ, 673, L155
Valenti S. et al., 2008b, MNRAS, 383, 1485
Valenti S. et al., 2009, Nat, 459, 674
Valenti S. et al., 2011, MNRAS, 416, 3138
Valenti S. et al., 2012, ApJ, 749, L28
Waldman R., Sauer D., Livne E., Perets H., Glasner A., Mazzali P., Truran J. W., Gal-Yam A., 2011, ApJ, 738, 21
Yaron O., Gal-Yam A., 2012, PASP, 124, 668
Yuan F., Kobayashi C., Schmidt B. P., Podsiadlowski P., Sim S. A., Scalzo R. A., 2013, MNRAS, 432, 1680

APPENDIX A: TABLES

Table A1. Optical photometry of SN 2012hn (Vega magnitudes in Landolt system)[a].

Date	JD − 240 0000	Phase[b]	*U*	*B*	*V*	*R*	*I*	Source[c]
2012-04-13	560 31.56	− 2.9	21.561 (200)	19.800 (042)	17.980 (050)	17.310 (027)	16.790 (020)	NTT
2012-04-15	560 32.56	− 1.9	–	19.944 (141)	17.903 (054)	17.286 (066)	16.751 (032)	PROMPT 5
2012-04-17	560 34.56	0.0	–	–	17.975 (065)	17.272 (079)	16.686 (053)	PROMPT 5
2012-04-18	560 35.50	1.0	–	–	18.074 (039)	17.294 (047)	16.736 (047)	PROMPT 5
2012-04-21	560 38.55	4.0	–	20.443 (268)	18.277 (073)	17.393 (089)	16.741 (051)	PROMPT 5
2012-04-20	560 38.58	4.1	–	20.490 (037)	18.206 (027)	17.450 (021)	16.720 (018)	NTT
2012-04-22	560 40.49	6.0	–	20.620 (237)	18.397 (083)	17.570 (102)	16.891 (053)	PROMPT 5
2012-04-23	560 40.53	6.0	22.282 (200)	20.800 (054)	18.320 (030)	17.540 (025)	16.830 (031)	NTT
2012-04-29	560 47.56	13.1	–	21.510 (064)	19.050 (072)	18.080 (027)	17.290 (036)	NTT
2012-04-30	560 48.48	14.0	–	21.530 (078)	19.020 (050)	18.160 (043)	17.320 (039)	NTT
2012-05-19	560 66.98	32.5	–	–	19.936 (045)	18.952 (039)	–	TRAPPIST
2012-05-19	560 66.98	32.5	–	–	–	–	18.026 (031)	PROMPT5
2012-05-19	560 67.50	33.0	–	22.210 (032)	19.951 (031)	–	–	DUPONT
2012-08-10	561 49.91	115.4	–	–	–	21.029 (035)	–	NTT
2012-08-25	561 64.87	130.4	–	–	22.683 (160)	21.354 (023)	20.427 (020)	NTT
2012-09-09	561 80.89	146.4	–	–	23.431 (560)	21.716 (286)	20.932 (250)	NTT
2012-10-16	562 17.81	183.3	–	–	23.762 (270)	22.514 (256)	21.721 (174)	NTT
2012-11-15	562 46.73	212.2	–	–	–	22.838 (083)	22.005 (081)	NTT
2012-12-04	562 65.82	231.3	–	–	–	23.020 (204)	–	NTT
2012-12-06	562 67.81	233.3	–	–	–	23.470 (217)	22.607 (145)	NTT

[a]The errors are computed taking into account both the uncertainty of the PSF fitting of the SN magnitude and the uncertainty due to the background contamination (computed by an artificial-star experiment). [b]Relative to the *R*-band maximum (JD = 245 6034.5). [c]PROMPT = PROMPT Telescopes and CCD camera Alta U47UV E2V CCD47-10; pixel scale = 0.590 arcsec pixel^{-1}. NTT = New Technology Telescope and EFOSC2; pixel scale = 0.24 arcsec pixel^{-1}. TRAPPIST = TRAnsiting Planets and PlanetesImals Small Telescope and FLI CCD; pixel scale = 0.64 arcsec pixel^{-1}. DUPONT = 2.5-m du Pont telescope and SITe2k; pixel scale = 0.259 arcsec pixel^{-1}.

Table A2. Optical photometry of SN 2012hn (AB magnitudes in Sloan system)[a].

Date	JD − 240 0000	Phase[b]	*g*	*r*	*i*	*z*	Source[c]
2012-04-14	560 31.51	− 3.0	18.367 (069)	–	–	–	NTT
2012-04-14	560 31.51	− 3.0	18.398 (138)	–	–	–	NTT
2012-04-15	560 32.59	− 1.9	–	17.667 (200)	–	–	PROMPT 5
2012-04-20	560 37.53	3.0	18.821 (085)	17.614 (092)	17.198 (061)	16.972 (039)	PROMPT 5/3
2012-04-21	560 38.52	4.0	18.882 (069)	–	–	–	NTT
2012-04-21	560 38.53	4.0	18.852 (066)	–	–	–	NTT
2012-04-24	560 41.48	7.0	19.276 (157)	17.760 (170)	–	–	PROMPT 5/3
2012-04-30	560 48.48	14.0	19.907 (110)	18.425 (071)	17.852 (025)	17.485 (035)	NTT

[a]The errors are computed taking into account both the uncertainty of the PSF fitting of the SN magnitude and the uncertainty due to the background contamination (computed by an artificial-star experiment). [b]Relative to the *R*-band maximum (JD = 245 6034.5). [c]PROMPT = PROMPT Telescopes and CCD camera Alta U47UV E2V CCD47-10; pixel scale = 0.590 arcsec pixel^{-1}. NTT = New Technology Telescope and EFOSC2; pixel scale = 0.24 arcsec pixel^{-1}.

Table A3. Optical photometry of SN 2012hn reference stars (Vega magnitudes in the Landolt system)[a].

Id	*U*	*B*	*V*	*R*	*I*
1	16.909 (068)	16.346 (021)	15.454 (017)	14.941 (020)	14.453 (017)
2	17.390 (033)	17.400 (053)	16.783 (065)	16.424 (074)	16.000 (073)
3	17.565 (043)	17.075 (059)	16.207 (089)	15.724 (083)	15.231 (091)
4	20.813 (026)	19.532 (068)	17.905 (163)	16.420 (107)	14.637 (085)
5	16.323 (025)	16.326 (060)	15.781 (083)	15.471 (086)	15.109 (059)
6	17.873 (074)	17.921 (029)	17.461 (053)	17.161 (053)	16.833 (026)
7	17.258 (051)	16.907 (005)	16.064 (020)	15.593 (031)	15.110 (024)
8	15.594 (035)	15.613 (011)	15.002 (024)	14.639 (029)	14.275 (045)
9	19.894 (075)	18.684 (046)	17.210 (029)	16.248 (023)	15.160 (032)
10	16.912 (046)	16.990 (035)	16.467 (070)	16.135 (063)	15.777 (067)

[a]The uncertainties are the standard deviation of the mean of the selected measurements.

Table A4. Optical photometry of SN 2012hn reference stars (AB magnitudes in Sloan system)[a].

Id	*g*	*r*	*i*	*z*
1	15.74 (07)	15.15 (06)	14.89 (04)	14.71 (02)
2	16.86 (07)	16.48 (06)	16.31 (04)	16.27 (02)
3	16.41 (06)	15.79 (06)	15.52 (04)	15.41 (02)
4	18.36 (07)	16.85 (06)	15.30 (03)	14.39 (02)
5	15.82 (06)	15.49 (05)	15.40 (03)	15.38 (02)
6	17.52 (07)	17.26 (06)	17.22 (04)	17.19 (02)
7	16.28 (06)	15.75 (05)	15.51 (04)	15.42 (02)
8	15.12 (06)	14.79 (05)	14.64 (03)	14.59 (02)
9	17.89 (07)	16.66 (06)	15.78 (04)	15.32 (02)
10	16.51 (07)	16.17 (06)	16.06 (04)	16.05 (02)

[a]The uncertainties are the standard deviation of the mean of the selected measurements.

This paper has been typeset from a TEX/LATEX file prepared by the author.